Cerebral Cortex Advance Access published May 2, 2007

Cerebral Cortex
doi:10.1093/cercor/bhm031

Differential Gene Expression between Sensory Neocortical Areas: Potential Roles for *Ten_m3* and *Bcl6* in Patterning Visual and Somatosensory Pathways

Catherine A. Leamey[1,2,3], Kelly A. Glendining[2], Gabriel Kreiman[1], Ning-Dong Kang[1], Kuan H. Wang[3,4], Reinhard Fassler[5], Atomu Sawatari[2], Susumu Tonegawa[3,4] and Mriganka Sur[1,3]

[1]Department of Brain and Cognitive Sciences, Massachusetts Institute of Technology, Cambridge MA 02139, USA, [2]Physiology, School of Medical Sciences and Bosch Institute, University of Sydney, Sydney NSW 2006, Australia, [3]Picower Institute for Learning and Memory and [4]Department of Biology, Massachusetts Institute of Technology, Cambridge MA 02139, USA and [5]Department of Molecular Medicine, Max-Planck Institute for Biochemistry, Martinsreid, Germany

Adult neocortical areas are characterized by marked differences in cytoarchitecture and connectivity that underlie their functional roles. The molecular determinants of these differences are largely unknown. We performed a microarray analysis to identify molecules that define the somatosensory and visual areas during the time when afferent and efferent projections are forming. We identified 122 molecules that are differentially expressed between the regions and confirmed by quantitative polymerase chain reaction 95% of the 20 genes tested. Two genes were chosen for further investigation: *Bcl6* and *Ten_m3. Bcl6* was highly expressed in the superficial cortical plate corresponding to developing layer IV of somatosensory cortex at postnatal day (P) 0. This had diminished by P3, but strong expression was found in layer V pyramidal cells by P7 and was maintained until adulthood. Retrograde tracing showed that *Bcl6* is expressed in corticospinal neurons. *Ten_m3* was expressed in a graded pattern within layer V of caudal cortex that corresponds well with visual cortex. Retrograde tracing and immunostaining showed that *Ten_m3* is highly expressed along axonal tracts of projection neurons of the developing visual pathway. Overexpression demonstrated that *Ten_m3* promotes homophilic adhesion and neurite outgrowth in vivo. This suggests an important role for *Ten_m3* in the development of the visual pathway.

Keywords: arealization, cortex, development, microarray, somatosensory, visual

Introduction

The adult cortex comprises discrete areas associated with distinct functions. Each area is characterized by unique patterns of cytoarchitecture, connectivity within and between cortical and subcortical regions, and functional roles. Recent work has provided strong evidence (reviewed in Sur and Rubenstein 2005) that factors both intrinsic and extrinsic to the cortex regulate the patterning and connectivity of cortical areas.

During early cortical development, secreted molecules such as bone morphogenic proteins, fibroblast growth factors (FGFs), and Wnt proteins are released from signaling centers at the margins of the developing cortical mantle (Shimogori et al. 2004). These morphogens are believed to act in a concentration-dependent manner and cause the graded activation or repression of transcription factors in the proliferative ventricular zone. The molecules responsible for the generation of the abrupt boundaries in cytoarchitecture and connectivity characteristic of the mature cortex are likely to include not only transcription factors but also cell surface and secreted molecules that directly guide the formation of connections. Indeed, mutations of the transcription factors Emx2 and Pax6, or alterations in FGF8 signaling, lead to changes in the expression of transcription factors (Tbr1, Id3, and COUP-TfI), axon guidance (ephrinA5 and EphA7), and adhesion molecules (cadherins 6 and 8) (Bishop et al. 2000; Mallamaci et al. 2000; Fukuchi-Shimogori and Grove 2001; Garel et al. 2003; Hamasaki et al. 2004; Shimogori and Grove 2005).

Interactions between membrane-bound molecules are thought to directly regulate numerous aspects of cortical organization and connectivity. Mutations in ephrinA5 lead to inappropriate innervation of somatosensory cortex by limbic thalamic nuclei (Bear et al. 1985; Uziel et al. 2002), and mutations in ephrinA5 and EphA4 lead to disruption of topography and areal specificity of thalamocortical projections (Dufour et al. 2003). The topographic specificity of cortico-thalamic projections is dependent on EphA7 (Torii and Levitt 2005). Mutations of ephrinA5 or EphA7 lead to a decrease in the size of somatosensory cortex (Miller et al. 2006), and several features of primary visual cortex are impaired in ephrinA2/A3/A5 triple mutants (Cang et al. 2005). A member of the L1 family of cell adhesion molecules is required for the development of normal cytoarchitecture in the visual cortex (Demyanenko et al. 2004).

Given the remarkable complexity of the cerebral cortex, it seems likely that a number of molecules, many as yet unknown, will play fundamental roles in establishing its exquisite patterns of connectivity. We reasoned that such molecules are likely to be differentially expressed between cortical areas at the time when corticopetal and corticofugal projections are forming. We thus performed a screen to identify molecules that are differentially expressed between 2 major sensory neocortical regions, primary somatosensory and visual areas, in newborn mice. We report the results of this analysis and the confirmation of a number of differentially expressed genes. Of particular interest, we report differential expression of 3 members of the Ten_m/Odz family of transmembrane proteins and show that at least one of these, *Ten_m3*, is expressed in an area and layer-specific pattern by projection neurons of the developing visual system. In addition, we show that *Bcl6*, a transcriptional repressor, is expressed by specific projection neurons in the somatosensory cortex.

Methods

All studies were performed on C57/Black6 mice and were approved by the animal ethics committees of Massachusetts Institute of Technology (MIT) and/or the University of Sydney.

Expression Analysis

Mice within 24 h of birth, designated postnatal day (P) 0, were anesthetized on ice, decapitated, and the brains removed. Curettes

(1 mm diameter) were used to isolate tissue from the somatosensory and visual cortices. Tissue from 2 to 3 litters (12 or more animals) was pooled for each pair of samples. Three pairs of samples were independently prepared and processed. The target regions for dissection were determined from preliminary experiments where tracer injections into cortical regions resulted in successful labeling of somatosensory or visual thalamus. Tissue was collected in RNAlater (Ambion, Foster City, CA). In some cases, tissue was stored in this solution at 4 °C for 1–2 days before further processing. Total RNA was extracted using Trizol (Invitrogen, Carlsbad, CA) and purified using the RNeasy kit (Qiagen, Valencia, CA) according to the manufacturers' instructions. The RNA was used to synthesize cDNA using superscript choice (Invitrogen) and a T7-dT(24) primer. The resulting DNA was purified using a phase lock gel (Eppendorf, Hamburg, Germany) and used as a template to produce biotinylated cRNA using an in vitro transcription reaction (Enzo, New York, NY). The resulting samples were purified using an RNeasy column and fragmented. The samples were hybridized to Affymetrix mouse U74v2 microarrays at the MIT biopolymer facility using standard Affymetrix protocols for hybridization, washing, staining, and scanning. These arrays contain 36 902 transcripts spanning the mouse genome.

Data were analyzed using the MAS5 statistical package (Affymetrix). Genes were analyzed according to 3 citeria: 1) A pairwise analysis was performed using Affymetrix software. Genes that showed an appropriate absence or presence call in all 3 repeats of each sample and an increase/decrease or marginal increase/decrease in 6 or more of the 9 comparisons between the 3 pairs were listed as potential candidates. 2) The fold change was calculated as the ratio of mean expression levels for each gene between the 2 regions. A minimum threshold for fold change was set at 1.4. 3) A significance analysis of microarrays (SAM) (Tusher et al. 2001) was performed. For this, a relative difference score for each gene was determined as the ratio between the difference in mean expressions levels for the 2 regions divided by the variance of the samples plus a constant which was calculated to minimize variation (equations are as described in Tusher et al. 2001). This score is essentially a measure of the signal to noise ratio and was thus used to rank the genes for significance. SAM analysis compares delta values, defined as the difference between the observed (actual) relative difference score compared with the mean of that obtained from 100 iterations of a random mixing of the samples (expected score). The threshold of delta was set at 1.2. To be considered as candidates for further analysis, we required genes to fulfill 2 or more of these criteria; in addition, a minimum cutoff for the relative difference score of 1.5 was applied. Two sets of genes were produced—those that were more highly expressed in visual cortex compared with somatosensory and those that were more highly expressed in somatosensory cortex compared with visual.

Confirmation of Differential Expression

The differential expression of the genes was confirmed using quantitative real-time reverse transcription polymerase chain reaction (PCR), using RNA samples from P0 somatosensory and visual cortex. The RNA samples used for confirmation were obtained independently from those used in the microarray analysis to provide an additional verification of the results. RNA was extracted and purified from P0 somatosensory and visual cortices as above, and first strand cDNA was synthesized using Superscript Reverse Transcriptase (Promega, Madison, WI) according to the manufacturer's instructions. Primers were designed to produce an amplicon of around 200 base pairs to ensure optimal reaction efficiency and sufficient fluorescence for detection. Primers were designed using Netprimer (PREMIER Biosoft International, www. Premierbioft.com) and Primer3 software (Rozen and Skaletsky 2000), based on the mRNA sequence entries in Genbank (primer sequences and accession numbers listed in Table 1 of the Supplementary Material). All primers were selected to have an annealing temperature of approximately 60 °C. Primer specificity was established by comparison with known genomes and sequences using the BLAST program (http://www.ncbi.nlm.nih.gov). PCR conditions were optimized on a Gradient PCR Cycler (Hybaid, Madison, WI) with respect to primer concentration, $MgCl_2$ concentration, and annealing temperature. Real-time PCR was performed using a Rotor-Gene 3000™ Real-Time Thermal Cycler (Corbett Life Technologies, Mortlake, NSW, Australia), and the amplification was monitored by SYBR green fluorescence (Morrison et al. 1998). Reactions were prepared in thin-walled PCR tubes using 2× Brilliant SYBR Green QPCR Master Mix (Stratagene, La Jolla, CA). On completion of the amplification cycles, a dissociation (melting) curve analysis (65–95 °C) was performed to control for nonspecific signal. All samples were analyzed in triplicate, with "no-template" controls included for each primer pair to test for template contamination of reaction reagents.

Levels of target gene transcripts were normalized to transcript levels of a reference gene (*GAPDH*) and calculated using a relative quantification model with efficiency correction (Pfaffl 2001). Amplification efficiency of primer pairs was calculated from serial dilutions of

Table 1

Genes identified here as being differentially expressed between somatosensory and visual cortex whose differential expression has been confirmed in neonatal mouse here and/or in other studies

Gene name	Symbol	Region	Confirmation provided by
Teneurin 3	*Ten_m3*	V	+, #, Li et al. (2006)
Teneurin 2	*Ten_m2*	V	+, Li et al. (2006)
Neuropilin 1	*Nrp1*	V	+
Mu-crystallin	*Crym*	V	+, *
T-shirt 3	*Tshz3*	V	+
COUP-Tf1	*Nr2f1*	V	Zhou et al. (2001)
Neurogenic differentiation 1	*NeuroD1*	V	*
Teneurin 4	*Ten_m4*	V	*, Li et al. (2006)
Dickkopf 3	*Dkk3*	V	+
EphrinA5	*Efna5*	S	Fukuchi-Shimogori and Grove (2001); Miller et al. (2006)
T brain 1	*Tbr1*	S	Bulfone et al. (1995); Miyashita-Lin et al. (1999)
RAR orphan receptor beta	*RORb/Nr1f2*	S	Miyashita-Lin et al. (1999); Fukuchi-Shimogori and Grove (2001)
Lim only domain 4	*Lmo4*	V	+, Bulchand et al. (2003)
Fibronectin leucine rich 3	*Flrt3*	V	+
Immunoglubulin superfamily 4/syncam	*Igsf4a*	V	+
AI838057	AI838057	V	+
B-cell leukemia 6	*Bcl6*	S	+, #, *
Dual specificity phosphatase 6	*Dusp6*	S	+
Transforming growth factor beta receptor 1	*TGFbR1*	S	+, *
Protein tyrosine phosphatase receptor O	*PTPrO*	S	+
Neuropeptide Y	*NPY*	S	+, *
Kelch repeat and BTB domain 9	*Kbtbd9*	S	+
Leucine zipper protein 2	*Luzp2*	S	+
Lim only domain 3	*Lmo3*	S	+, Bulchand et al. (2003)
Ubiquitin specific phosphatase 6	*Usp6*	S	+

Note: +, genes confirmed here by PCR; #, genes confirmed here by in situ hybridization and/or immunohistochemistry; *, reported as differentially expressed in manner similar to that found here by Funatsu et al. (2004) or Sansom et al. (2005), but the difference in regions and/or ages (E11, E13, or E16 vs. P0) sampled prevents this from being used as direct confirmation of our data.

a representative cDNA template over a concentration range of 3 log orders (data not shown), using the equation $E = 10^{[-1/slope]}$ (Rasmussen 2001). Statistical analysis was performed using the relative expression software tool (REST 2005 BETA V1.9.12) (Pfaffl et al. 2002) and pairwise fixed reallocation randomization test (Pfaffl et al. 2004). Differences were considered significant at a level of $P < 0.05$.

Investigation of Spatial and Temporal Expression Patterns of Selected Candidates

Differential expression of selected genes was also confirmed using in situ hybridization and/or immunohistochemistry. For in situ hybridization, 200-bp long sense and anti-sense dioxygenin (DIG)–labeled riboprobes were synthesized and hybridized to15-μm thick cryostat sections of fresh frozen brain tissue using standard techniques. Staining was developed using peroxidase-tagged anti-DIG Fab fragments (Roche, Indianapolis, IN) and a tyramide signal amplification (TSA) kit (Perkin-Elmer, Waltham, MA). For immunohistochemistry, either 15 μm cryostat sections were prepared from fresh frozen tissue and postfixed in 4% paraformaldehyde or animals were anesthetized with an overdose of sodium pentobarbital and perfused with 0.9% saline followed by 4% paraformaldehyde in 0.1 M sodium phosphate buffer (PB; pH 7.4), and 50-μm thick sections were prepared on the freezing microtome. Rabbit anti-Ten_m3 antibody (Zhou et al. 2003) was diluted 1:50 in 0.1 M PB containing 2% normal goat serum and 0.1% Triton-X, and sections were incubated overnight at 4 °C. Following incubation in a biotinylated goat anti-rabbit secondary antibody, ABC (Vector, Burlingame, CA; 1:100) staining was developed using a TSA kit as above.

For retrograde tracing experiments, animals were anesthetized by inhalation of 2–4% isofluorane in oxygen and 1% choleratoxin subunit B (CTB) conjugated to alexa fluor 594 (Molecular Probes, Carlsbad, CA) was pressure-injected into superior colliculus, spinal cord, or cortex using a picospritzer. Following 2 days transport, animals were sacrificed, brains removed, and tissue processed for in situ hybridization as above. For transneuronal tracing, animals were anesthetized as above and 5% wheat germ agglutin conjugated to horseradish peroxidase (WGA–HRP) was injected intraocularly at P2–3. Following transport times of 3 days, animals were perfused with 10% glycerol, the brains were frozen and processed for immunohistochemistry on fresh frozen sections as above. A rabbit anti-WGA antibody (Sigma, San Diego, CA) was used at 1:1000 and reaction signal developed as for Ten_m3.

Overexpression of Ten_m3

The full-length *Ten_m3* construct was cloned from partial cDNA sequences for mouse *Ten_m3* (Oohashi et al. 1999). They were inserted into the pCAGGS mammalian expression vector upstream of an internal ribosomal entry site–green fluorescent protein (IRES–GFP) site from the eGFP vector (Clontech, Mountain View, CA). The IRES–GFP site was also inserted into the pCAGGS vector on its own to act as a control. In preliminary experiments, the efficacy of the constructs was tested on primary cultures of dissociated cortical neurons. Transfection was achieved using Lipofectamine (Invitrogen) according to the manufacturer's instructions. In utero electroporation was performed as described (Saito and Nakatsuji 2001). Timed pregnant mice were anesthetized in 2–4% isofluorane, and an abdominal incision was made to expose the uterus. Plasmid DNA was pressure-injected into the lateral ventricle under visual control, and 5× 50 ms 35 V pulses were applied to the head region across the uterine wall using paddle electrodes. Embryos were returned to the abdominal cavity, and mothers typically gave birth naturally. Animals were euthanized and perfused with 4% paraformaldehyde, and coronal sections were prepared on the freezing microtome. In some cases, the GFP signal was amplified with a rabbit anti-GFP antibody (Abcam, Cambridge, UK) 1:500 followed by a goat anti-rabbit secondary antibody conjugated to alexa fluor 488.

Quantification of Images

Two or 3 images through the peak of the labeling each from 3 different *GFP* and *Ten_m3-GFP*-transfected animals (a total of 7 sections from *GFP* controls and 8 sections from *Ten_m3-GFP* cases) were analyzed quantitatively. Images were converted to 8-bit tagged image files. Background was subtracted in Image J (the National Institutes of Health [NIH]) using a rolling ball radius of 500. Brightness and contrast levels were normalized in Photoshop (Adobe), and the resultant images were thresholded in Image J. The pixel coordinates for each image were written to text files that were further processed using the image analysis toolbox in Matlab where the size of labeled patches was measured in pixels. In order to be considered in the analysis, patches had to exceed a minimum size of 60 pixels. This threshold was chosen as it approximates the smallest regions that were clearly identifiable as cells in our images. One pixel is approximately equivalent to 0.6 μm^2. Mean patch size, maximum patch size, and the number of patches exceeding thresholds of 200, 350, 500, and 1000 pixels were calculated to identify patches of label corresponding to multiple cells. Statistical analysis was performed using the Wilcoxon rank-sum test.

Results

Gene Expression in Visual and Somatosensory Cortex

Microarray Analyses

The complete data set showing expression values for all the genes is posted at the Web site http://www.physiol.usyd.edu.au/~cathy/. Genes were analyzed according to 3 criteria: the pairwise comparison of increase/decrease calls, fold change, and the relative difference score (see Methods). The pairwise comparison gave a list of 145 transcripts that fulfilled this criterion. The expression values for these transcripts in comparison to the entire population are plotted in Figure 1*a*, and the complete list is available at the Web site. Of these, 45 were upregulated in visual cortex in comparison to somatosensory cortex, and the remainder were upregulated in somatosensory in comparison to visual cortex. Genes were also analyzed for mean fold change. A threshold of 1.4 was chosen, and it was found that 1050 transcripts fulfilled this criterion. Their expression values are plotted in Figure 1*b*, and the genes are listed at the Web site given above. A SAM was also performed using a delta threshold of 1.2. The plot of relative versus expected values of the relative difference scores is shown in Figure 1*c*. The expression values for the 44 genes that fulfilled this criterion are indicated on the scatter plot in Figure 1*d* and are listed at the Web site.

The three lists of transcripts identified by each method were partially overlapping and corresponded to a total of 1091 transcripts. The lists obtained from each method reflect the biases of each selection procedure (see Discussion). In the interests of maximizing sensitivity while minimizing false discovery rates (FDRs), it was decided to combine these forms of analysis. For follow-up analysis, we required that genes fulfill at least 2 of the 3 criteria used here and, in addition, exceed a minimum threshold of 1.5 for their relative difference score. We found that 135 transcripts fulfilled these criteria, including 11 genes that were identified by all analysis criteria (SAM, pairwise comparison, and fold change). The complete list of genes upregulated in visual and somatosensory cortices, along with their expression values, is available at the Web site; the expression values for these genes are also plotted in Figure 1*e*. Of these 135 transcripts, 51 were upregulated in visual cortex and 84 were upregulated in somatosensory cortex. A number of the transcripts identified corresponded to genes that were represented multiple times on the microarray, leaving a total of 122 differentially expressed molecules, comprising 45 (32 genes and 13 expressed sequence tags) which were more highly expressed in samples from visual cortex and 77 (60 genes and 17 ESTs) which were more highly expressed in samples from somatosensory cortex. A heat map indicating the relative

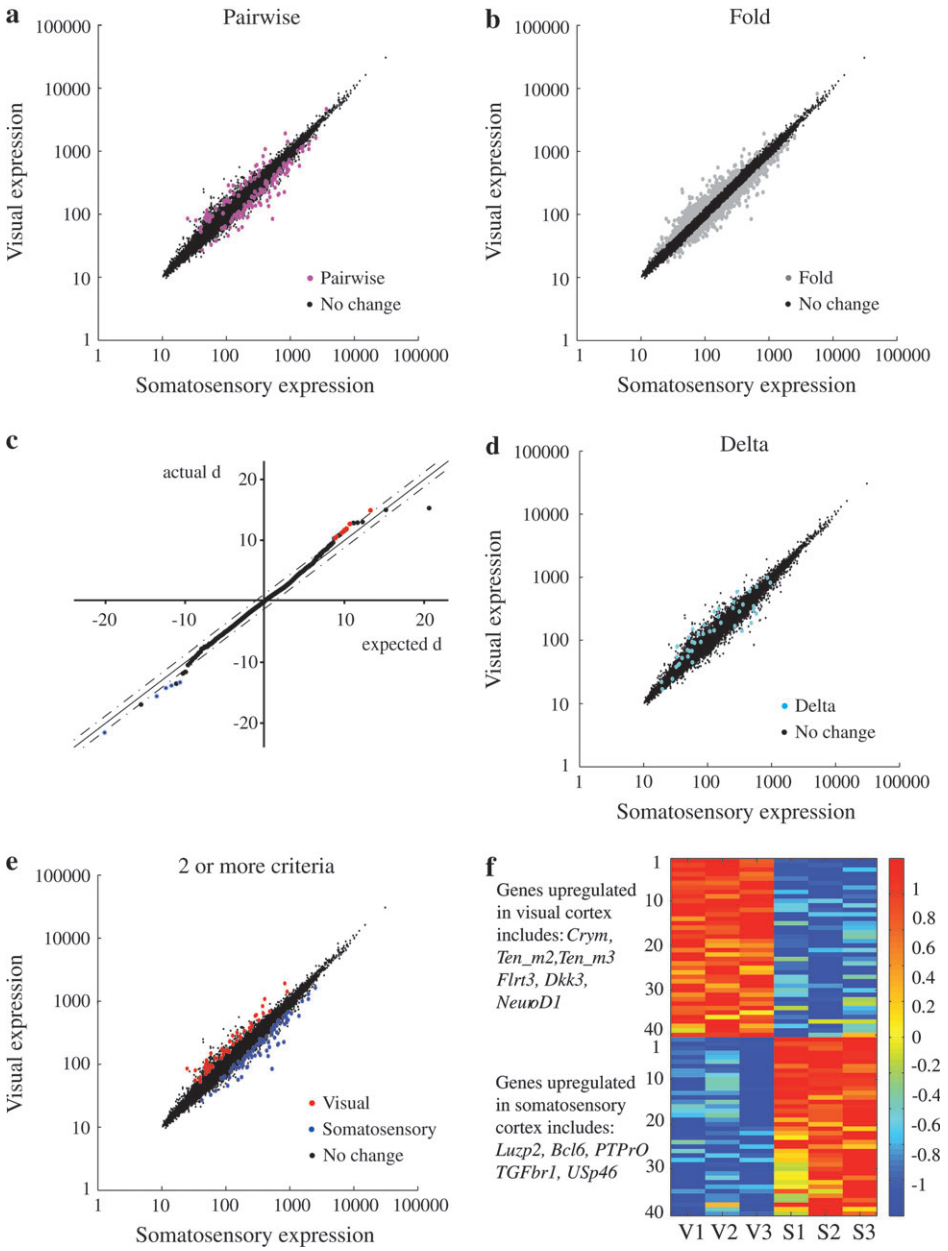

Figure 1. Graphs plotting results of microarray screen. (*a*, *b*, *d*) Mean expression values for all genes in somatosensory and visual cortex. Genes that did not fulfill a given criterion are plotted in black. Genes identified using the pairwise comparison (*a*), mean fold change (*b*), and SAM analysis (*d*) are highlighted, respectively. (*c*) Results of the SAM analysis showing actual versus expected values of the relative difference score. Genes that exceeded delta = 1.2 fall outside the dotted lines. Those that passed the SAM analysis and also fulfilled at least one of the other 2 criteria are highlighted in red for visual and blue for somatosensory cortex. (*e*) The 135 transcripts that fulfilled at least 2 of the 3 criteria and exceeded a minimum cutoff for the relative difference score of 1.5 are highlighted in red for visual cortex and blue for somatosensory. These are the transcripts considered for follow-up analysis. (*f*) Heat map showing relative expression across the 3 repeats of each pair of samples from somatosensory and visual cortex for the top 40 differentially genes, as ranked by relative difference score, which fulfilled 2 or more analysis criteria.

expression of the top 40 transcripts from each area as ranked by the relative difference score is shown in Figure 1*f*.

The identified genes included several that have previously been reported to be differentially expressed between somatosensory and visual cortex in early postnatal animals, such as ephrinA5, *COUP-TfI (Nr2f1)*, *ROR*β, Tbr1, *Lmo3*, and *Lmo4* (Miyashita-Lin et al. 1999; Fukuchi-Shimogori and Grove 2001; Zhou et al. 2001; Bulchand et al. 2003; Garel et al. 2003). In addition, *NeuroD1*, *Ten_m4*, *Bcl6*, *mu-crystallin (Crym)*, and *TGF*β*r1* have been reported to be differentially expressed between cortical regions at earlier developmental stages (Funatsu et al. 2004; Sansom et al. 2005). Although this cannot be taken as direct confirmation of our results due to the different ages sampled, the expression patterns previously reported are consistent with those found here. Together, the data indicate success of the assay and analysis method in identifying differentially expressed genes. In addition, a large number of genes not previously reported as being differentially expressed were also identified. These included a number of transcription factors including *Bhlbh2*, *Foxp1*, *Lbd2*, and *Luzp2*. A number of genes associated with axon guidance such as neuropilin 1 (*Nrp1*), semaphorins 3C and 7A, and protein tyrosine phosphatase

receptor O (*PTPrO*), which has recently been shown to modulate Eph receptor activity (Shintani et al. 2006), were identified as well. Table 1 provides a summary of the genes identified here as differentially expressed that have been confirmed either here (see below) or in other studies.

Molecules associated with specific morphogen signaling pathways, for example, 3 molecules associated with the transforming beta growth factor (TGFβ) pathway—TGFβ receptor 1 (*TGFβr1*), Mad homolog 1 (*Smad1*), and zinc finger homeobox b1 (*Zfhxb1*) transcription factor—were all upregulated in somatosensory cortex. Phosphorylation of *TGFβr1* signals Smad proteins to translocate to the nucleus where they activate transcription (reviewed in Charron and Tessier-Lavigne 2005). Fibronectin leucine-rich transmembrane protein 3 (*Flrt3*) and Dickkopf 3 (*Dkk3*) were both upregulated in visual cortex. *Flrt3* is associated with FGF signaling and can promote homophilic adhesion and neurite outgrowth (Tsuji et al. 2004; Haines et al. 2006; Karaulanov et al. 2006). *Dkk3* is member of the Dickkopf family, which are secreted regulators of Wnt signaling (Brott and Sokol 2002). Although typically associated with the regulation of cell fate, a number of morphogens have recently been shown to also play roles in axon guidance (Charron and Tessier-Lavigne 2005). A number of adhesion molecules including pCAS130 (*BCar1*), immunoglobulin superfamily member 4a (*Igsf4a* or Syncam), cadherin 4, protcadherins 9 and 17, and plakophilin 4 were differentially expressed. Also of interest was the fact that 3 teneurin genes (*Ten_m/Odz 2*, *3*, and *4*), which encode members of a family of transmembrane proteins, were all identified as being more highly expressed in visual cortex than somatosensory. Another recent study has also implicated these genes in arealization by showing that they may act downstream of Emx2 in defining caudal cortical regions (Li et al. 2006).

Real-Time PCR Analyses

Real-time PCR was used to confirm differential gene expression. Twenty genes and ESTs (10 each from somatosensory and visual cortical regions) that correspond to a total of 27 identified transcripts (20% of the total number of transcripts identified) and that spanned the range of values for fold change (from 1.4 to 6.2) and relative difference scores (from 1.7 to 21) were chosen. Genes chosen were predominantly not those previously reported as differentially expressed so as to provide novel data; a few of those previously reported were included as an independent control, however. Many of the genes chosen are associated with developmental processes and/or encode cell surface or extracellular proteins. All of the genes tested showed higher expression in the cortical region from which they were identified, consistent with the microarray analysis, and for 19 of the 20 genes, the differences were statistically significant ($P < 0.05$; pairwise fixed random reallocation test). The results are presented in Figure 2. The gene tested for which a significant difference in expression between the samples from somatosensory and visual cortex was not found was opioid cell adhesion molecule (*Opcm1/Obcam*). The fact that 19 of the 20 genes (corresponding to 25 of the 27 transcripts) tested here were confirmed as significantly different, in addition to a number which have been independently confirmed by other studies (see above), indicates that the analysis used here reliably identified differentially expressed genes. In some cases, the fold change as determined by real-time PCR was notably higher

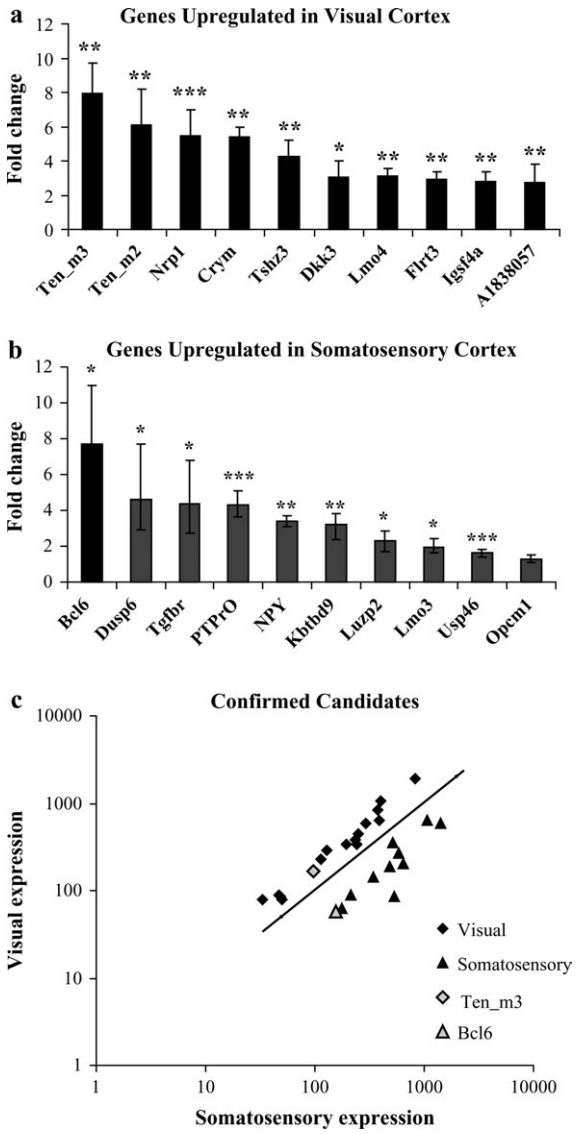

Figure 2. Confirmation of differential expression by quantitative real-time PCR. (*a*, *b*) Fold change in expression values between samples from somatosensory and visual cortex for selected genes is plotted (mean ± standard error). Ten genes that were identified as being more highly expressed in visual (*a*) or somatosensory (*b*) cortex were investigated. All showed expression patterns consistent with the region in which higher expression was detected by the microarray analysis. Almost all showed a statistically significant difference in expression between the 2 samples. $*P < 0.5$; $**P < 0.01$; $***P < 0.001$. (*c*) Mean expression values for the 25 transcripts, corresponding to the 19 genes confirmed by real-time PCR in this study, are shown. The genes found to be most highly differentially expressed in each cortical region, *Ten_m3* (visual) and *Bcl6* (somatosensory), are highlighted.

than that suggested by the microarray. For example, it was found that *Ten_m3* and *Bcl6*, which had mean fold changes of 1.7 and 2.7, respectively, according to the microarray analysis, both had fold changes of almost 8-fold according to the real-time PCR analysis. The observation that fold change as determined by the microarray analysis in many cases underestimated the fold change determined by quantitative PCR was also made in a recent survey of differences in gene expression between cortical neuron subtypes (Sugino et al. 2006). A plot showing the expression values as determined by the microarray analysis for the transcripts confirmed here and which highlights *Ten_m3* and *Bcl6* is shown in Figure 2*c*.

Bcl6 Expression

Based on this analysis, 2 genes were selected for further investigation of their spatiotemporal expression patterns: *Ten_m3* and *Bcl6*. Each of the genes met the microarray criteria for differential expression and had the highest quantitative PCR expression levels of all analyzed visual or somatosensory cortex genes. *Bcl6* is a transcription repressor, mutations of which are associated with B-cell lymphomas (Ye et al. 1993). In situ hybridization for *Bcl6* confirmed the differential expression of this gene along the rostrocaudal axis of the neocortex at P0, with strong expression in the superficial region of the cortical plate in a position that is consistent with the position of the developing somatosensory cortex (Fig. 3*a*). Expression was strongest in the superficial region of the cortical plate that corresponds predominantly to layer IV cells at this stage of development (Caviness 1982) though some fainter expression was also seen deep to this in the developing layer V. Importantly, no expression was seen in caudal neocortex corresponding to the position of visual cortex. Expression was, however, also seen in hippocampus, subiculum, and globus pallidus. The mediolateral distribution of label seen in a coronal section also corresponds well to layer IV of somatosensory cortex (Fig. 3*b*).

To determine whether the differential expression of *Bcl6* expression is maintained at later developmental stages, expression in older animals was also investigated. At P3, expression in the somatosensory cortex had decreased to a level that was barely detectable using this technique (not shown) although expression was clearly visible in the hippocampus and subiculum of the same sections, suggesting the lack of expression in somatosensory cortex reflected a real decrease in expression levels in this region. Expression at P7 was strikingly different with expression in a subset of neurons in layer V of the rostral 2/3 of cortex (Fig. 3*c*). Strong expression was also present in the CA1 region of hippocampus and the subiculum. The robust expression in layer V was maintained in the adult. Interestingly, expression appeared to be associated with large pyramidal cells, suggesting the gene may be associated with large projection neurons in layer V. To investigate this possibility, retrograde tracing from the spinal cord, a major target of layer V pyramidal cells from the rostral 2/3 of cortex, was performed at P10 and analyzed at P14. The results of this analysis are presented in Figure 4. It was found that many of the retrogradely labeled corticospinal neurons (Fig. 4*a*) also expressed *Bcl6* (Fig. 4*a′*,*a″*). Thus, *Bcl6* is expressed by long-range projection neurons in layer V.

Ten_m3 Expression

We also investigated the expression pattern of *Ten_m3*. *Ten_m3* belongs to a family of 4 homodimeric transmembrane proteins (Oohashi et al. 1999; Feng et al. 2002). In situ hybridization confirmed the results of the microarray analysis and revealed a remarkably restricted expression of *Ten_m3* in the caudal region of cortex that correlates well with the position of developing visual cortex (Fig. 5*a*). Interestingly, expression was restricted not only in terms of region but also with respect to layer and was seen predominantly in the developing layer V (this is the region immediately deep to the densely packed undifferentiated superficial region of the cortical plate which contains mostly layer IV cells at this stage; Caviness 1982; Auladell et al. 2000). Immunostaining for *Ten_m3* demonstrated that the protein showed a similar

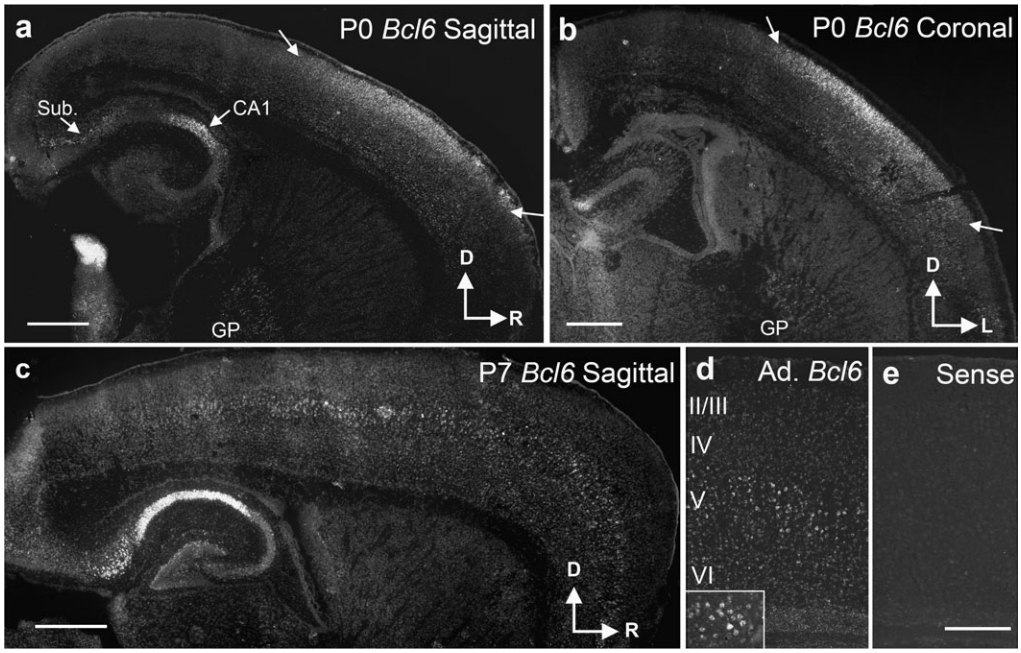

Figure 3. In situ hybridization for *Bcl6* confirms differential expression. (*a*) Sagittal section through somatosensory cortex at P0 confirms high expression in this region compared with more caudal cortex. In situ signal is highest in the superficial layer of the cortical plate that corresponds predominantly to the cells of the developing layer IV at this stage. Fainter signal is also observed in layers V and VI. Strong expression is also seen in a subregion of the CA1 region of hippocampus, subiculum (Sub.), and globus pallidus (GP). (*b*) A coronal section through somatosensory cortex at P0 shows that mediolateral expression of *Bcl6* is consistent with the position of somatosensory cortex. Faint expression is also observed more laterally. (*c*) A sagittal section at P7 shows a very different pattern of expression. No signal above background is observed in layer IV though robust signal is observed in a subset of layer V neurons. (*d*) Expression in layer V neurons is maintained in the adult. Inset shows that morphology is consistent with that of pyramidal projection neurons. (*e*) Sense control from a section adjacent to that in (*d*) demonstrating specificity of the signal. Scale bars: (*a*, *b*) 600 μm; (*c*) 800 μm; (*e*) 250 μm, also applies to (*d*) and corresponds to 100 μm in the inset. Orientations as marked, D: dorsal; R: rostral; L: lateral.

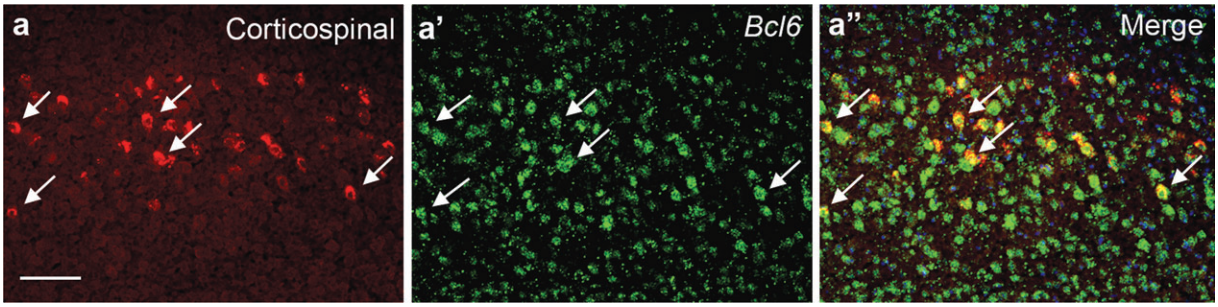

Figure 4. *Bcl6* is expressed in corticospinal neurons by P14. (*a*) Corticospinal neurons retrogradely labeled with CTB injected into the thoracic spinal cord at P10. (*a′*) The same section as in a photographed to reveal the in situ hybridization signal for *Bcl6*. (*a″*) An overlay of (*a′*) and (*a″*) shows that all of the retrogradely labeled corticospinal neurons express high levels of *Bcl6*. Arrows highlight the same cells in all 3 images. Scale bar: 100 μm.

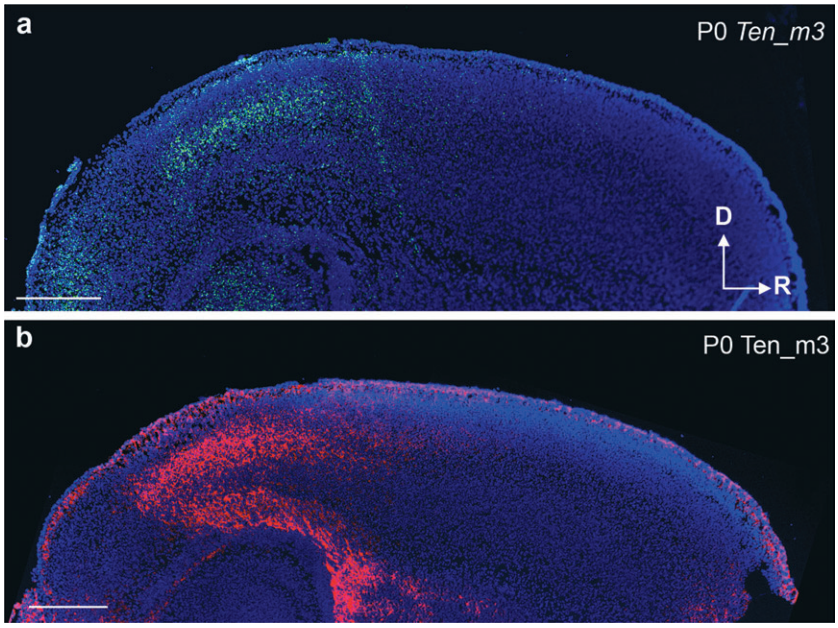

Figure 5. *Ten_m3* expression pattern confirms microarray analysis. (*a*) In situ hybridization for *Ten_m3* (green) in a sagittal section at P0 In situ signal (green) is shown superimposed on a fluorescent nuclear counterstain (blue). Expression is highly localized to caudal cortex that corresponds well to the position of visual cortex. The signal is further localized to developing layer V. (*b*) Immunostaining for *Ten_m3* from a nearby section to that shown in (*a*) confirms that the protein is expressed by cells in layer V of caudal cortex. Fine bands of label are also visible in layer VI, and label in the developing white matter suggests that the protein is expressed on axons growing to and/or from visual cortex. Scale bars: 500 μm. D: dorsal; R: rostral.

distribution in terms of rostrocaudal extent as revealed by the in situ hybridization, but in addition to the staining in layer V, thin strands of label were seen to transverse layer VI and strong staining was seen in the intermediate zone (white matter) and in the internal capsule (Fig. 5*b*). Together, these results suggest that *Ten_m3* is expressed along the axons of cells projecting from the visual cortex. Because *Ten_m3* was also observed in the dorsal lateral geniculate nucleus at this stage (not shown but see Fig. 6*a*), the immunostaining observed in the white matter may also reflect expression of *Ten_m3* along geniculocortical axons.

We further investigated the expression pattern of *Ten_m3* using in situ hybridization during the first postnatal week (Fig. 6). A similar pattern of expression to that seen at P0 was observed in sagittal sections at P3 with high expression in layer V of caudal cortex (Fig. 6*a,b*). At this stage of development, pale staining could also be barely discerned in layer IV of slightly more rostral cortex that likely corresponds to the developing somatosensory cortex (see inset Fig. 6*a*). This was much fainter than that seen in caudal cortex, however. Expression was also observed in the dLGN, subiculum, and a subregion of CA1; patches of staining were seen in the striatum. Strong staining was also seen in the medial entorhinal cortex (not shown). We wished to determine how the expression of *Ten_m3* correlates with the visual cortex. For this, transneuronal tracing with WGA–HRP was performed to label geniculocortical terminals (Fig. 6*c*). The rostrocaudal distribution of label in the cortex corresponded remarkably well the region of strong expression in layer V of caudal cortex, suggesting that visual cortex does indeed express the gene. Interestingly, we also observed that there appears to be a gradient of *Ten_m3* expression in visual cortex that is highest caudally and diminishes rostrally (Fig. 6*a*). We also examined *Ten_m3* staining in coronal sections and again found that the distribution corresponded well with visual cortex, though some label was also observed more laterally suggesting that the gene may be expressed by more lateral regions including area 18 (Fig. 6*d,e*). The expression pattern described above was maintained until at least P7, but had begun to decline by P14 (not shown). Faint expression was observed in both layers V and VI of caudal cortex in the adult (not shown but see, e.g., the Allen Brain Atlas: http://www.brain-map.org/welcome.do).

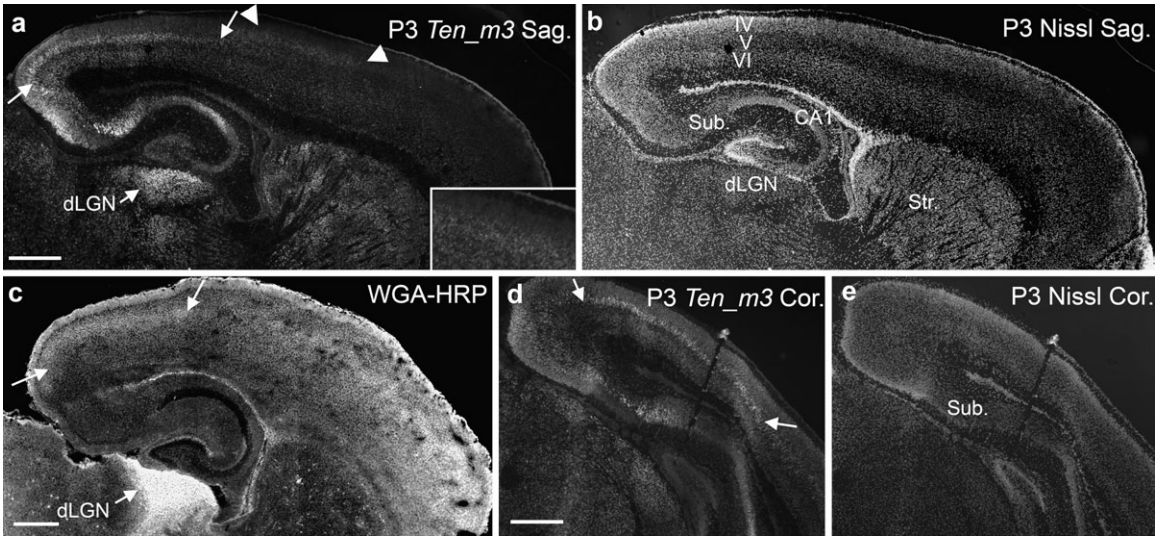

Figure 6. *Ten_m3* expression is maintained during the first postnatal week. (*a*) In situ hybridization for *Ten_m3* in a sagittal section at P3. A fluorescent nuclear stain for the same section is shown in (*b*). High expression is maintained in layer V of caudal cortex (approximate boundaries indicated by small arrows) where it appears to be in a high caudal to low rostral gradient. Expression is also high in dLGN (arrow). By this stage, faint expression can just be discerned in layer IV of slightly more rostral cortex consistent with the position of somatosensory cortex (arrowheads). This region is shown in more detail in the inset. High expression is also visible in subiculum (Sub.), a subregion of CA1, and patches within striatum (Str.). (*c*) Transneuronal labeling of the geniculocortical projection (small arrows) shows that the rostrocaudal extent of projections from visual thalamus matches well with the distribution of *Ten_m3* expression within caudal cortex, suggesting that *Ten_m3* is expressed in visual cortex. (*d–e*) In situ hybridization for *Ten_m3* (*d*) and corresponding fluorescent nuclear stain (*e*) in a coronal section through visual cortex at P3. The mediolateral distribution of *Ten_m3* staining correlates well with visual cortex although expression is also seen in more lateral regions suggesting that it may also be expressed in area 18 and other caudolateral cortex. Scale bars: 600 μm in (*a–e*) represents 250 μm in inset of (*a*).

We wished to determine if *Ten_m3* is expressed by projection neurons of layer V. To do this, we labeled cells retrogradely from structures that are major output targets of layer V of visual cortex, the ipsilateral superior colliculus and the contralateral visual cortex, and performed in situ hybridization for *Ten_m3* (Fig. 7). Following injections of a retrograde tracer (CTB) into the superior colliculus, most of the labeled neurons expressed *Ten_m3* clearly above background levels, thus suggesting that the gene is expressed by corticocollicular projection neurons (Fig. 7*a–a′′*). Retrograde tracing of another major output of layer V, the callosal projection, produced more equivocal results. The labeled callosal neurons were not *Ten_m3* positive, suggesting the gene may be differentially expressed between these populations (Fig. 7*b–b′′*). Given the nature of this analysis, however, it is not possible to definitively determine whether this is a consistent difference between the populations of neurons. Injections of CTB into visual cortex also resulted in labeling in dLGN (Fig. 7*c*). Although we cannot rule out the possibility that a proportion of this label represents corticogeniculate terminals, its appearance is strongly suggestive of somata and primary dendrites, which also express *Ten_m3* (Fig. 7*c′*), indicating that geniculocortical neurons also express *Ten_m3* (Fig. 7*c′′*). These results therefore indicate that *Ten_m3* is expressed in one or more subsets of projection neurons of the developing visual system, including the corticocollicular projection and the geniculocortical projections.

Ten_m3 and Cell Adhesion

No functional role has been reported for *Ten_m3*, although other members of the *Ten_m* gene family encode transmembrane glycoproteins that are homophilic and homodimeric (Oohashi et al. 1999; Feng et al. 2002; Rubin et al. 2002), suggesting that *Ten_m3* may also mediate cell adhesion. As a first step to determining a role for *Ten_m3* in vivo, we examined the effects of localized overexpression of the gene using in utero electroporation. The full-length *Ten_m3* construct was cloned into a mammalian expression vector downstream of an IRES–GFP site. The same vector with the IRES–GFP site only was used as a control. In preliminary experiments, *GFP*-only or *Ten_m3–GFP* was transfected into primary dissociated cortical cultures; in situ hybridization (not shown) and immunostaining revealed that *Ten_m3* was being produced by the transfected cells. Confocal analysis revealed that *Ten_m3* was being appropriately targeted to the membrane (Fig. 8*a–a′′*).

In utero electroporation was used to transfect neurons in neocortex. Transfection with the control GFP-only construct on E14 resulted in the presence of a large cohort of GFP positive cells in layer IV (Fig. 8*b,c*). Transfection with *Ten_m3–GFP* typically resulted in GFP positive cells that appeared markedly different compared with *GFP* transfection alone (Fig. 8*d,e*). Rather than cells that were distributed in a seemingly random fashion within the transfected region as in controls, cells transfected with *Ten_m3–GFP* were typically grouped in clumps or clusters. At higher power, it can be seen that these clusters consist of groups of GFP positive somata (Fig. 8*e*) and their processes that are also intertwined. This effect was very consistent and markedly different from controls, where cells and their processes are clearly separate from each other. The effect on cellular clustering was quantified by measuring the size of GFP positive patches in thresholded images. Three parameters—mean patch size, maximum patch size, and the number of patches greater than threshold value which was larger than an average patch of label from control animals (the latter was treated both as an absolute number and as a proportion of the total number of patches)—were significantly greater ($P < 0.01$; Wilcoxon rank-sum test) from material from animals transfected with *Ten_m3–GFP* compared with *GFP* controls. These results are presented in Table 2. The clustering of cells made it difficult to ascertain whether there were also changes in the

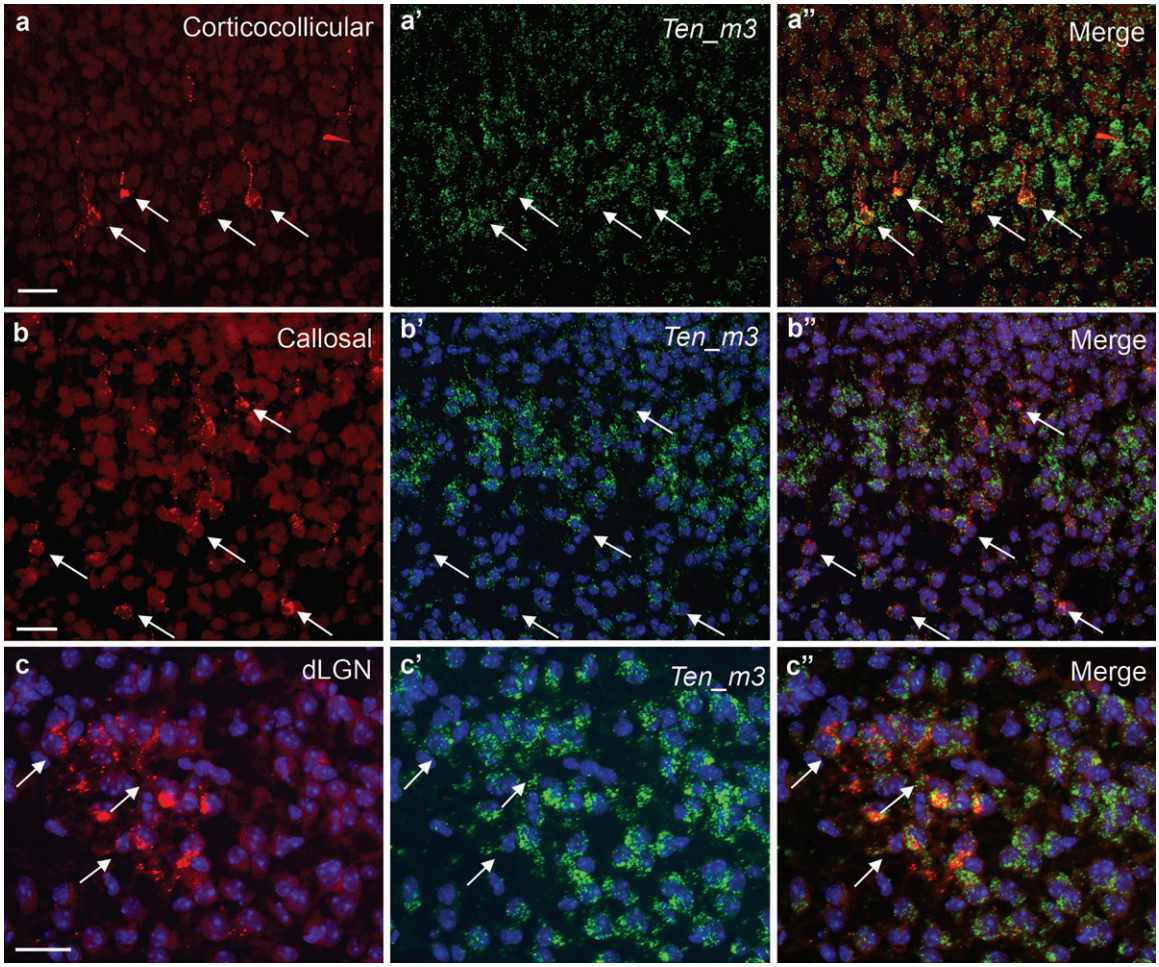

Figure 7. *Ten_m3* is expressed in projection neurons of the developing visual system. (*a–a″*) Section through visual cortex at P5 photographed to show retrogradely labeled corticocollicular neurons (*a*) and *Ten_m3* mRNA (*a′*). The images are merged in (*a″*) to show the relationship between the staining patterns. The same cells are indicated by arrows in all 3 images. The retrogradely labeled corticocollicular neurons are highly *Ten_m3* positive. (*b–b″*) As for (*a–a″*), but following retrograde labeling of the callosal projection. Retrogradely labeled callosal neurons (*b*) are not highly *Ten_m3* positive (*b′*, *b″*). (*c–c″*) Section through the dLGN showing that retrogradely labeled geniculocortical neurons (*c*) express *Ten_m3* (*c′*, *c″*). In some cells, highlighted by arrows, *Ten_m3* mRNA and the retrograde tracer can be seen in primary dendritic processes. Scale bars: 25 μm.

morphology of individual neurons at this stage of development. A case where *Ten_m3-GFP* was transfected at E13 to target layer V cells is shown in Figure 8*f*. Again cells and their processes are clustered together. In this instance, where very large numbers of cells were transfected, the migration of the GFP positive neurons seems to have been delayed. This is evidenced by the fact that, unlike control cases where transfected cells are all aligned within a distinct lamina by P8 (Fig. 8*b*), in *Ten_m3-GFP*-transfected cases (Fig. 8*d–f*), some labeled cells are still present in the ventricular zone. In Figure 8*f*, numerous clusters of labeled cells are clearly visible throughout the depth of the cortex, suggesting that these cells are still migrating to their destination. We suggest that this delay is probably a consequence of the overexpression of an adhesive molecule rather than an indication that Ten_m3 normally plays a major role in neural migration. These results are consistent with the suggestion that Ten_m3 promotes adhesive interactions between cells that express it.

The long-term effects of overexpression of Ten_m3 were also examined in animals that were transfected at E15 and allowed to survive till adulthood. Although GFP was barely visible under the fluorescence microscope at this stage, immunostaining for GFP revealed that the protein was still present in significant quantities in material from control (Fig. 9*a,b*) and *Ten_m3-GFP*-transfected (Fig. 8*c,d*) animals. There was no evidence of inappropriate laminar positioning of cells at this stage, suggesting that if migration had been affected in these animals that it had not impacted the final position of the cells to any significant degree. The prominent clustering apparent at early stages was also not apparent. There was however a dramatic increase in the number of labeled neurites visible in the material from *Ten_m3-GFP*-transfected mice compared with controls. This is most apparent at high power (compare Fig. 9*b,d*). Due to the high density of labeled processes in *Ten_m3*-GFP–transfected material, it was not possible to reliably quantify changes in morphology at the single neuron level. Instead, quantification of the changes in neurite outgrowth was performed at the population level. This was based on a threshold analysis of labeled material in each image which showed that there was an almost 3-fold increase in the proportion of the image that contained labeled cells and processes in *Ten_m3-GFP*-transfected animals (38.9 ± 9.3%; mean ± standard deviation [SD] for $n = 8$ sections from 2 animals) compared with GFP alone (13.5 ± 5.6%; mean ± SD

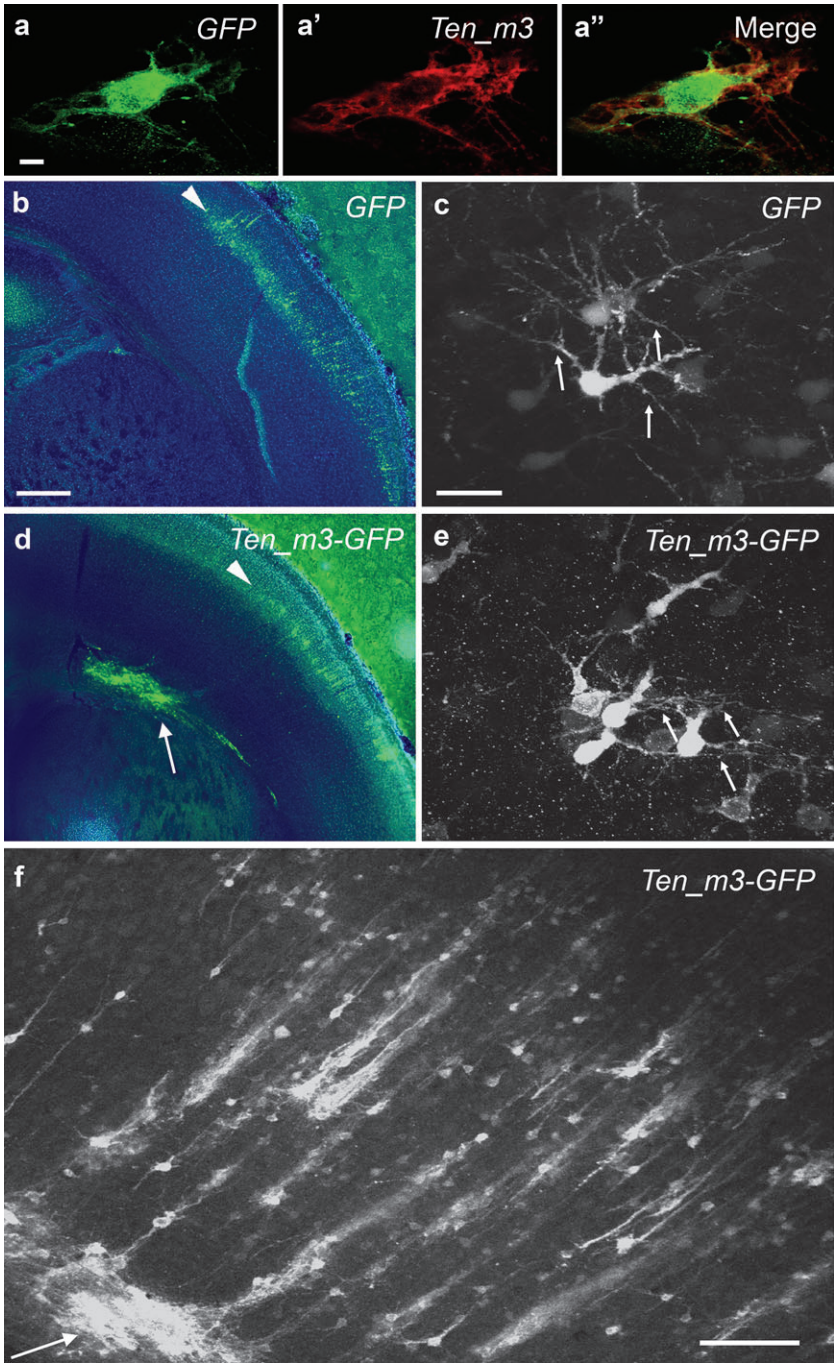

Figure 8. Effects of transfection of *Ten_m3*. (*a–a″*) Confocal section through a cell transfected in vitro with *Ten_m3–GFP* showing GFP (*a*) immunoreactivity for *Ten_m3* (*a′*) and a merged image of the two (*a″*). GFP is predominantly expressed in the cytosol, whereas *Ten_m3* (*a′*) is expressed in the membrane. (*b–e*) Coronal sections through rostral cortex at P8 from animals transfected at E14 to target layer IV showing the distribution of cells transfected with *GFP*-only (*b*, *c*) or *Ten_m3–GFP* (*d*, *e*). Low power (*b*, *d*) views of GFP (green) superimposed on a fluorescent couterstain (blue) and high power (*c*, *e*) views are shown. In material from *Ten_m3-GFP*–transfected animals, cells are grouped into clusters. At high power, it is seen that these clusters comprise groups of neurons and their processes that are intertwined (arrows in *d*). This is quite distinct from the appearance of cells and their processes in GFP-only–transfected animals, where cells appear to be uniformly distributed within the transfected area, and the process of nearby cells remain clearly separate (arrows in *c*). In GFP-transfected animals, all labeled cells are aligned in a layer within the cortex (arrowhead in *b*). In *Ten_m3-GFP*–transfected cases, whereas some cells have migrated to a similar position as seen for controls (arrowhead in *d*), others are still in the ventricular zone (arrow in *d*). (*f*) A large transfection on E13 targeting layer V shown here at P8. There is a tight clustering of cells and their processes. Some cells are still located in the ventricular zone (arrow), whereas other are scattered throughout the depth of the cortex suggesting that migration of many neurons has been delayed. Scale bars: (*a*) 10 μm; (*b*) 200 μm, applies to (*d*); (*c*) 40 μm, applies to (*e*); (*f*) 100 μm.

for $n = 8$ sections from 2 animals). This difference ($P < 0.05$; *t*-test) is not due to differences in the numbers of labeled cells in the images, which were almost identical between the 2 sets of images: the thresholded proportion of each image per transfected cell was 3.3 ± 1.4 for control and 9.3 ± 1.5 for *Ten_m3-GFP*-transfected cases ($P < 0.05$; *t*-test). Qualitatively, similar effects on neurite outgrowth were observed regardless of area or layer transfected, suggesting that Ten_m3 can strongly promote neurite outgrowth in many types of neurons.

Table 2

Quantification of the effect of *Ten_m3* on cellular clustering in cortical cells from P7–8 mice that were transfected with *GFP*-only or *Ten_m3–GFP* in utero

Parameter	GFP control	*Ten_m3–GFP*	Probability
Mean patch size	182.6 ± 15.0	499.5 ± 56.4	$P < 0.001$
Maximum patch size	1579 ± 303	16237 ± 3142	$P < 0.01$
Number patches > threshold	7.7 ± 2.1	22.9 ± 3.2	$P < 0.01$
Percentage patches > threshold	8.4 ± 1.8%	18.6 ± 1.4	$P < 0.01$

Note: Numbers represent numbers of pixels (mean ± standard error) that appear as a continuous patch when thresholded from images through the peak of the *GFP* or *Ten_m3–GFP* transfections. A pixel represents approximately 0.6 μm^2. Two or 3 sections each from 3 different animals were quantified in each case. Probabilities were calculated using the Wilcoxon rank-sum test. Thresholds for the data shown here were set at 500 pixels, 2–3 times larger than average patch size in control animals to identify clustered cells. Significantly different results for the *GFP* and *Ten_m3-GFP*–transfected cases groups were also obtained for thresholds set at 200, 350, and 1000 pixels. All measurements show patch size is significantly higher in material from *Ten_m3-GFP*–transfected cases compared with control, suggesting that *Ten_m3-GFP*–transfected cells are clustered much more frequently than *GFP*-transfected cells.

Discussion

The aim of this study was to identify genes that are differentially expressed between neocortical areas in neonatal mice. The day of birth was chosen because this is a time when many corticopetal and corticofugal projections—some of the key defining features of the nascent cortical areas—are forming. The 122 molecules identified here are thus candidates for playing a role in this process or other aspects of cortical organization. The success of our approach is indicated by the presence of most molecules previously reported to be differentially expressed between rostral and caudal cortex in neonatal mice in our list of candidate genes. The differential expression between cortical areas of many of the genes identified here is novel, however, and we anticipate that this will provide a useful framework for investigations of molecular determinants of cortical patterning and connectivity. It was not feasible to study the spatiotemporal expression of all the candidates. Our PCR data, however, strongly suggest that a large proportion of the genes identified here are indeed differentially expressed. Further, the results obtained for *Bcl6* and *Ten_m3* demonstrate that genes identified are differentially expressed between somatosensory and visual cortex. The expression pattern of *Ten_m3* within visual cortex makes it a particularly strong candidate for future studies.

Microarray Analysis

The ability to perform rapid genome-wide screens is enormously powerful yet presents its own difficulties, particularly in terms of analysis. Standard statistical tests, such as the *t*-test, are not reliable when applied to 3–4 repeats of around 36 000 transcripts. The SAM was developed to circumvent some of these difficulties (Tusher et al. 2001) and has been used successfully by recent studies (Sansom et al. 2005; Tropea et al. 2006). This analysis is highly effective at identifying genes with low variability in their absolute expression levels across replicates as determined by the microarray analysis but tends to miss transcripts with variability in absolute expression even if they show consistent relative changes. In addition, the sample preparation and analysis procedures are not immune to error. Thus, the application of stringent criteria based on variability will tend to miss significant numbers of genes that are differentially expressed. Reducing the stringency of the criteria in an unbiased manner will however increase the FDR to high levels (Tusher et al. 2001). The pairwise comparison is sensitive to changes in relative expression levels between pairs of samples from different regions but tends to miss small changes. Fold change gives a measure of the relative expression levels but does not take variability between replicates into account. Consequently, it was decided to combine these approaches and require genes to fulfill at least 2 of the 3 criteria in combination with a minimum cutoff for the relative difference score. This proved highly successful at identifying differentially expressed transcripts, with 95% of genes tested confirmed as differentially expressed. Although similarly high success levels may have been achieved using the SAM analysis alone, many genes whose differential expression was confirmed (e.g., *Ten_m3*, *Ten_m2*, *Bcl6*, *Lmo4*) would have been missed unless the SAM criteria were dropped to levels corresponding to >50% FDR. In a study where Affymetrix criteria were used on their own, only around 50% of the identified genes were confirmed (Funatsu et al. 2004). We suggest that the combination of these forms of analysis provides a reliable and sensitive approach.

In addition to the microarray analysis, a major potential source of error here is the accuracy of the dissections. The regions chosen were based on preliminary tracing experiments that labeled appropriate thalamic nuclei. The confirmation of expression patterns by in situ hybridization suggests these were largely accurate. The possibility that cortical regions adjacent to somatosensory and visual cortex may have been included in some dissections cannot however be excluded. Although we estimate that 90% or more of the tissue included was indeed from the target regions, it is possible that some of the genes identified here may be differentially expressed between occipital and parietal regions rather than visual and somatosensory cortices per se. Because the development of the visual cortex is delayed with respect to the development of the somatosensory cortex by around 1 day in rodents (Bayer and Altman 1991), it is possible that some of the genes identified could reflect developmental rather areal differences. Our assay used tissue containing heterogeneous populations of cells. It is possible, therefore, that some differences between subtypes of cells from different areas may have been masked. The fact that we identified genes which are differentially expressed within specific laminae suggests that our assay was sufficiently sensitive to detect neurons differentially expressed within specific layers; it would be of interest to further refine this study to investigate lamina or neuron subtype specific differences (Arlotta et al. 2005; Christophe et al. 2005; Sugino et al. 2006) between cortical areas during development.

The validity of our analysis is supported not only by the fact that almost all of the genes whose differential expression was tested were confirmed but also by the presence of most genes previously found to be differentially expressed between rostral and caudal neonatal cortex in our screen. These include *ROR*β, Tbr1, ephrinA5, *COUP-Tf1*, *Lmo3*, and *Lmo4* (Miyashita-Lin et al. 1999; Fukuchi-Shimogori and Grove 2001; Zhou et al. 2001; Bulchand et al. 2003; Garel et al. 2003). There are however a few genes that seem conspicuous by their absence, most notably cadherin 8 (*Cad8*) and EphA7. Although EphA7 is consistently reported as expressed in visual cortex, its expression is not limited to this region (Miller et al. 2006) and shows a graded expression pattern within visual cortex (Cang et al. 2005). *Cad8* has been used by a number of studies as a marker for visual cortex (Fukuchi-Shimogori and Grove 2001; Hamasaki et al. 2004; Cang et al. 2005), so its absence in our analysis was of

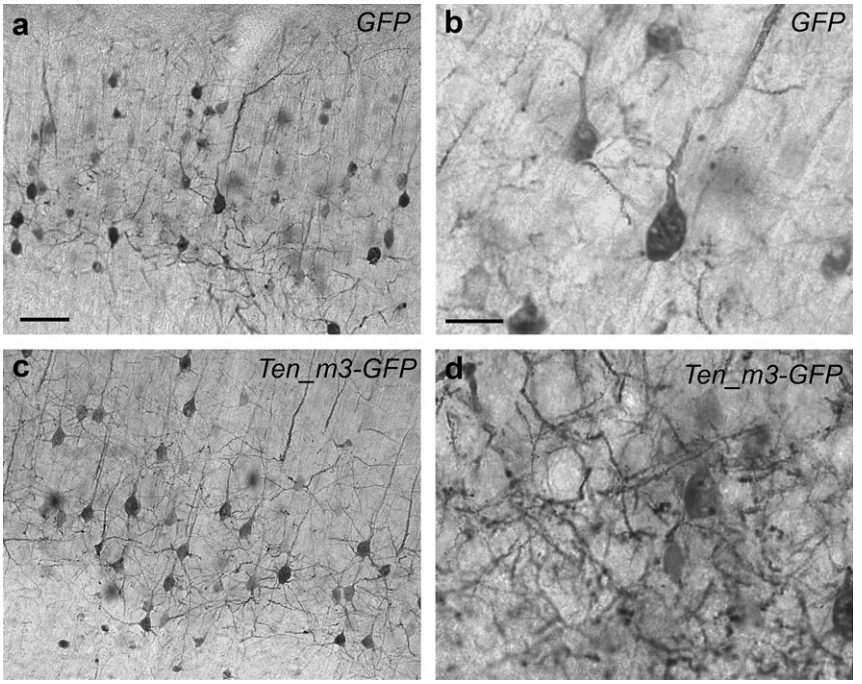

Figure 9. (*a–d*) GFP immunostaining in low (*a*, *c*) and high (*b*, *d*) power images of sections through cortex from adult mice that were transfected with *GFP* (*a*, *b*) or *Ten_m3–GFP* (*c*, *d*) in utero. Although similar numbers of cells are labeled in each image, there is a dramatic increase in neurite outgrowth in material from *Ten_m3*-transfected animals. This increase was highly consistent and was independent of region or layer transfected. Scale bars: (*a*) 50 μm, applies to (*c*); (*b*) 20 μm, applies to (*d*).

some concern. However, data presented in a recent study (Miller et al. 2006) show a surprisingly uniform distribution of *Cad8* along the rostrocaudal axis of the cortex; its absence in our analysis is consistent with this.

The genes selected for confirmation by real-time PCR spanned a range of relative difference scores to test the validity of our analysis. Many of the genes tested were chosen because they encode cell surface or extracellular proteins and/or are associated with developmental processes. Of particular interest was the differential expression of genes associated with signaling pathways of morphogens as well as adhesion and axon guidance molecules (see Results). A few of the genes identified here were also reported in a microarray screen to identify genes differentially expressed between corticospinal, corticotectal, and callosal neurons (Arlotta et al. 2005), including *Bcl6* (see below). A few of the other genes identified here (*Lmo4*, *Crym*, *Dkk3*, and *S100a10*) were also identified by Arlotta et al. (2005); differences in experimental design make it difficult to make useful comparisons between the results.

Bcl6

Our demonstration that *Bcl6* is expressed in corticospinal neurons by P14 is consistent with the work of Arlotta et al. (2005). Our data also show, however, that expression of *Bcl6* in developing cortex is highly dynamic. A dynamic pattern of *Bcl6* expression has also been found in the olfactory epithelium (Otaki et al. 2005). These authors proposed that *Bcl6* may play a role in the terminal differentiation of olfactory sensory neurons consistent with its role in the differentiation of germinal center B cells (Dent et al. 1997; Fukuda et al. 1997; Ye et al. 1997). A role for this gene in cortical development is yet to be determined. The high level of expression of *Bcl6* in corticospinal neurons that is maintained into adulthood is particularly intriguing and warrants further investigation.

Ten_m3

Three members of the *Ten_m* family were identified as more highly expressed in visual cortex. The *Ten_ms* encode a highly conserved family of 4 type II transmembrane glycoproteins that are the vertebrate homologs (Oohashi et al. 1999) of the late-acting Drosophila pair-rule gene *Ten_m/Odz* (Baumgartner et al. 1994; Levine et al. 1994). Expression patterns in the developing mammalian embryo (Zhou et al. 2003) suggest important roles during early development. *Ten_ms 1* and *2* are expressed in complimentary patterns in the developing avian visual system, and roles in adhesion and neurite outgrowth have been reported in vitro (Rubin et al. 1999, 2002). Other studies have shown that the intracellular domains can be cleaved and translocate to the nucleus where interactions with zic1 (Bagutti et al. 2003) and methyl binding domain 1 and CAP/ponsin (Nunes et al. 2005) have been reported. The carboxy terminal has also been found to produce a neuromodulatory peptide (Wang et al. 2005; Tucker and Chiquet-Ehrismann 2006). This information, combined with the fact that *Ten_m3* showed the greatest fold change in expression between somatosenory and visual cortex in the real-time PCR analysis, led us to investigate the expression pattern and potential role of *Ten_m3* in some detail. A recent study has reported that *Ten_ms 2*, *3*, and *4* are downstream targets of Emx2 signaling (Li et al. 2006). Our independent discovery of their differential expression in visual cortex is largely in agreement with these observations and highlights the success of our screen in identifying previously unknown arealization candidates. Our characterization of *Ten_m3* also provides considerable novel data on this intriguing but currently little known family of molecules.

Our in situ hybridization and immunohistochemistry data show that *Ten_m3* is not only differentially expressed between somatosensory and visual cortex but also highly expressed by

specific subsets of neurons within this region, most notably the corticocollicular projection neurons of layer V of visual cortex. Our data also suggest that it is expressed by other projection neurons of the developing visual system, such as the geniculocortical projection. Most interestingly, immunohistochemistry showed that the protein is expressed along the trajectories of growing axons, suggesting a potential role in axon targeting. Our data also show that *Ten_m3* strongly promotes both homophilic adhesion and neurite outgrowth in vivo. To our knowledge, this represents the first demonstration of a role for any *Ten_m* in vivo in vertebrates. Together, these data suggest important roles for *Ten_m3*, and potentially other members of the *Ten_m* family, in mediating patterns of connectivity in the developing mammalian visual system.

Supplementary Material

Supplementary material can be found at http://www.cercor.oxfordjournals.org/.

Notes

Supported by grants from the NIH and the Simons Foundation (MS) and the National Health and Medical Research Council, Australia (CAL). We would like to acknowledge the assistance of Arvind Govindrajan in the in vitro testing of the constructs, the MIT Biopolymer facility for processing the microarrays, Drs Sharon Kolk and Maria Donoghue for advice on in utero electroporation and Serkan Oray for assistance with confocal microscopy. *Conflict of Interest*: None declared.

Address correspondence to Catherine A. Leamey, Department of Physiology, F13, University of Sydney, Sydney NSW 2006, Australia. Email: cathy@physiol.usyd.edu.au.

References

Arlotta P, Molyneaux BJ, Chen J, Inoue J, Kominami R, Macklis JD. 2005. Neuronal subtype-specific genes that control corticospinal motor neuron development in vivo. Neuron. 45:207–221.

Auladell C, Perez-Sust P, Super H, Soriano E. 2000. The early development of thalamocortical and corticothalamic projections in the mouse. Anat Embryol (Berl). 201:169–179.

Bagutti C, Forro G, Ferralli J, Rubin B, Chiquet-Ehrismann R. 2003. The intracellular domain of teneurin-2 has a nuclear function and represses zic-1-mediated transcription. J Cell Sci. 116:2957–2966.

Baumgartner S, Martin D, Hagios C, Chiquet-Ehrismann R. 1994. Tenm, a Drosophila gene related to tenascin, is a new pair-rule gene. Embo J. 13:3728–3740.

Bayer SA, Altman J. 1991. Neocortical development. New York: Raven.

Bear MF, Schmechel DE, Ebner FF. 1985. Glutamic acid decarboxylase in the striate cortex of normal and monocularly deprived kittens. J Neurosci. 5:1262–1275.

Bishop KM, Goudreau G, O'Leary DD. 2000. Regulation of area identity in the mammalian neocortex by Emx2 and Pax6. Science. 288:344–349.

Brott BK, Sokol SY. 2002. Regulation of Wnt/LRP signaling by distinct domains of Dickkopf proteins. Mol Cell Biol. 22:6100–6110.

Bulchand S, Subramanian L, Tole S. 2003. Dynamic spatiotemporal expression of LIM genes and cofactors in the embryonic and postnatal cerebral cortex. Dev Dyn. 226:460–469.

Bulfone A, Smiga SM, Shimamura K, Peterson A, Puelles L, Rubenstein JL. 1995. T-brain-1: a homolog of Brachyury whose expression defines molecularly distinct domains within the cerebral cortex. Neuron. 15:63–78.

Cang J, Kaneko M, Yamada J, Woods G, Stryker MP, Feldheim DA. 2005. Ephrin-as guide the formation of functional maps in the visual cortex. Neuron. 48:577–589.

Caviness VS Jr. 1982. Neocortical histogenesis in normal and reeler mice: a developmental study based upon [3H]thymidine autoradiography. Brain Res. 256:293–302.

Charron F, Tessier-Lavigne M. 2005. Novel brain wiring functions for classical morphogens: a role as graded positional cues in axon guidance. Development. 132:2251–2262.

Christophe E, Doerflinger N, Lavery DJ, Molnar Z, Charpak S, Audinat E. 2005. Two populations of layer v pyramidal cells of the mouse neocortex: development and sensitivity to anesthetics. J Neurophysiol. 94:3357–3367.

Demyanenko GP, Schachner M, Anton E, Schmid R, Feng G, Sanes J, Maness PF. 2004. Close homolog of L1 modulates area-specific neuronal positioning and dendrite orientation in the cerebral cortex. Neuron. 44:423–437.

Dent AL, Shaffer AL, Yu X, Allman D, Staudt LM. 1997. Control of inflammation, cytokine expression, and germinal center formation by BCL-6. Science. 276:589–592.

Dufour A, Seibt J, Passante L, Depaepe V, Ciossek T, Frisen J, Kullander K, Flanagan JG, Polleux F, Vanderhaeghen P. 2003. Area specificity and topography of thalamocortical projections are controlled by ephrin/Eph genes. Neuron. 39:453–465.

Feng K, Zhou XH, Oohashi T, Morgelin M, Lustig A, Hirakawa S, Ninomiya Y, Engel J, Rauch U, Fassler R. 2002. All four members of the Ten-m/Odz family of transmembrane proteins form dimers. J Biol Chem. 8:8.

Fukuchi-Shimogori T, Grove EA. 2001. Neocortex patterning by the secreted signaling molecule FGF8. Science. 294:1071–1074.

Fukuda T, Yoshida T, Okada S, Hatano M, Miki T, Ishibashi K, Okabe S, Koseki H, Hirosawa S, Taniguchi M, et al. 1997. Disruption of the Bcl6 gene results in an impaired germinal center formation. J Exp Med. 186:439–448.

Funatsu N, Inoue T, Nakamura S. 2004. Gene expression analysis of the late embryonic mouse cerebral cortex using DNA microarray: identification of several region- and layer-specific genes. Cereb Cortex. 14:1031–1044.

Garel S, Huffman KJ, Rubenstein JL. 2003. Molecular regionalization of the neocortex is disrupted in Fgf8 hypomorphic mutants. Development. 130:1903–1914.

Haines BP, Wheldon LM, Summerbell D, Heath JK, Rigby PW. 2006. Regulated expression of FLRT genes implies a functional role in the regulation of FGF signalling during mouse development. Dev Biol. 297:14–25.

Hamasaki T, Leingartner A, Ringstedt T, O'Leary DD. 2004. EMX2 regulates sizes and positioning of the primary sensory and motor areas in neocortex by direct specification of cortical progenitors. Neuron. 43:359–372.

Karaulanov EE, Bottcher RT, Niehrs C. 2006. A role for fibronectin-leucine-rich transmembrane cell-surface proteins in homotypic cell adhesion. EMBO Rep. 7:283–290.

Levine A, Bashan-Ahrend A, Budai-Hadrian O, Gartenberg D, Menasherow S, Wides R. 1994. Odd Oz: a novel Drosophila pair rule gene. Cell. 77:587–598.

Li H, Bishop KM, O'Leary DD. 2006. Potential target genes of EMX2 include Odz/Ten-M and other gene families with implications for cortical patterning. Mol Cell Neurosci. 33:136–149.

Mallamaci A, Muzio L, Chan CH, Parnavelas J, Boncinelli E. 2000. Area identity shifts in the early cerebral cortex of Emx2-/- mutant mice. Nat Neurosci. 3:679–686.

Miller K, Kolk SM, Donoghue MJ. 2006. EphA7-ephrin-A5 signaling in mouse somatosensory cortex: developmental restriction of molecular domains and postnatal maintenance of functional compartments. J Comp Neurol. 496:627–642.

Miyashita-Lin EM, Hevner R, Wassarman KM, Martinez S, Rubenstein JL. 1999. Early neocortical regionalization in the absence of thalamic innervation. Science. 285:906–909.

Morrison TB, Weis JJ, Wittwer CT. 1998. Quantification of low-copy transcripts by continuous SYBR Green I monitoring during amplification. Biotechniques. 24:954–958, 960, 962.

Nunes SM, Ferralli J, Choi K, Brown-Luedi M, Minet AD, Chiquet-Ehrismann R. 2005. The intracellular domain of teneurin-1 interacts with MBD1 and CAP/ponsin resulting in subcellular codistribution and translocation to the nuclear matrix. Exp Cell Res. 305:122–132.

Oohashi T, Zhou XH, Feng K, Richter B, Morgelin M, Perez MT, Su WD, Chiquet-Ehrismann R, Rauch U, Fassler R. 1999. Mouse ten-m/Odz is

a new family of dimeric type II transmembrane proteins expressed in many tissues. J Cell Biol. 145:563–577.
Otaki JM, Fearon DT, Yamamoto H. 2005. The proto-oncogene BCL-6 is expressed in olfactory sensory neurons. Neurosci Res. 53: 189–200.
Pfaffl MW. 2001. A new mathematical model for relative quantification in real-time RT-PCR. Nucleic Acids Res 29:e45.
Pfaffl MW, Horgan GW, Dempfle L. 2002. Relative expression software tool (REST) for group-wise comparison and statistical analysis of relative expression results in real-time PCR. Nucleic Acids Res. 30:e36.
Pfaffl MW, Tichopad A, Prgomet C, Neuvians TP. 2004. Determination of stable housekeeping genes, differentially regulated target genes and sample integrity: BestKeeper—Excel-based tool using pair-wise correlations. Biotechnol Lett. 26:509–515.
Rasmussen R. 2001. Quantification on the LightCycler. In: Meuer S, Wittwer C, editors. Rapid cycle real-time PCR, methods and applications. Heidelberg (Germany): Springer Press. p. 21–34.
Rozen S, Skaletsky H. 2000. Primer3 on the WWW for general users and for biologist programmers. Methods Mol Biol. 132:365–386.
Rubin BP, Tucker RP, Brown-Luedi M, Martin D, Chiquet-Ehrismann R. 2002. Teneurin 2 is expressed by the neurons of the thalamofugal visual system in situ and promotes homophilic cell-cell adhesion in vitro. Development. 129:4697–4705.
Rubin BP, Tucker RP, Martin D, Chiquet-Ehrismann R. 1999. Teneurins: a novel family of neuronal cell surface proteins in vertebrates, homologous to the Drosophila pair-rule gene product Ten-m. Dev Biol. 216:195–209.
Saito T, Nakatsuji N. 2001. Efficient gene transfer into the embryonic mouse brain using in vivo electroporation. Dev Biol. 240: 237–246.
Sansom SN, Hebert JM, Thammongkol U, Smith J, Nisbet G, Surani MA, McConnell SK, Livesey FJ. 2005. Genomic characterisation of a Fgf-regulated gradient-based neocortical protomap. Development. 132:3947–3961.
Shimogori T, Grove EA. 2005. Fibroblast growth factor 8 regulates neocortical guidance of area-specific thalamic innervation. J Neurosci. 25:6550–6560.
Shimogori T, VanSant J, Paik E, Grove EA. 2004. Members of the Wnt, Fz, and Frp gene families expressed in postnatal mouse cerebral cortex. J Comp Neurol. 473:496–510.
Shintani T, Ihara M, Sakuta H, Takahashi H, Watakabe I, Noda M. 2006. Eph receptors are negatively controlled by protein tyrosine phosphatase receptor type O. Nat Neurosci. 9:761–769.
Sugino K, Hempel CM, Miller MN, Hattox AM, Shapiro P, Wu C, Huang ZJ, Nelson SB. 2006. Molecular taxonomy of major neuronal classes in the adult mouse forebrain. Nat Neurosci. 9:99–107.
Sur M, Rubenstein JL. 2005. Patterning and plasticity of the cerebral cortex. Science. 310:805–810.
Torii M, Levitt P. 2005. Dissociation of corticothalamic and thalamocortical axon targeting by an EphA7-mediated mechanism. Neuron. 48:563–575.
Tropea D, Kreiman G, Lyckman A, Mukherjee S, Yu H, Horng S, Sur M. 2006. Gene expression changes and molecular pathways mediating activity-dependent plasticity in visual cortex. Nat Neurosci. 9:660–668.
Tsuji L, Yamashita T, Kubo T, Madura T, Tanaka H, Hosokawa K, Tohyama M. 2004. FLRT3, a cell surface molecule containing LRR repeats and a FNIII domain, promotes neurite outgrowth. Biochem Biophys Res Commun. 313:1086–1091.
Tucker RP, Chiquet-Ehrismann R. 2006. Teneurins: a conserved family of transmembrane proteins involved in intercellular signaling during development. Dev Biol. 290:237–245.
Tusher VG, Tibshirani R, Chu G. 2001. Significance analysis of microarrays applied to the ionizing radiation response. Proc Natl Acad Sci USA. 98:5116–5121.
Uziel D, Muhlfriedel S, Zarbalis K, Wurst W, Levitt P, Bolz J. 2002. Miswiring of limbic thalamocortical projections in the absence of ephrin-A5. J Neurosci. 22:9352–9357.
Wang L, Rotzinger S, Al Chawaf A, Elias CF, Barsyte-Lovejoy D, Qian X, Wang NC, De Cristofaro A, Belsham D, Bittencourt JC, et al. 2005. Teneurin proteins possess a carboxy terminal sequence with neuromodulatory activity. Brain Res Mol Brain Res. 133:253–265.
Ye BH, Cattoretti G, Shen Q, Zhang J, Hawe N, de Waard R, Leung C, Nouri-Shirazi M, Orazi A, Chaganti RS, et al. 1997. The BCL-6 proto-oncogene controls germinal-centre formation and Th2-type inflammation. Nat Genet. 16:161–170.
Ye BH, Lista F, Lo Coco F, Knowles DM, Offit K, Chaganti RS, Dalla-Favera R. 1993. Alterations of a zinc finger-encoding gene, BCL-6, in diffuse large-cell lymphoma. Science. 262:747–750.
Zhou C, Tsai SY, Tsai MJ. 2001. COUP-TFI: an intrinsic factor for early regionalization of the neocortex. Genes Dev. 15:2054–2059.
Zhou XH, Brandau O, Feng K, Oohashi T, Ninomiya Y, Rauch U, Fassler R. 2003. The murine Ten-m/Odz genes show distinct but overlapping expression patterns during development and in adult brain. Gene Expr Patterns. 3:397–405.